TECHNICAL RESEARCH REPORT

Randon Transforms, Wavelets, and Applications

by C. Berenstein

T.R. 96-65

Sponsored by
the National Science Foundation
Engineering Research Center Program,
the University of Maryland,
Harvard University,
and Industry

Radon transforms, wavelets, and applications

Carlos Berenstein

We present here the informal notes of four lectures[1] given at Cá Dolfin, Venice, under the auspices of CIME. They reflect the research of the author, his collaborators, and many other people in different applications of integral geometry. This is a vast and very active area of mathematics, and we try to show it has many diverse and sometimes unexpected applications, for that reason it would impossible to be complete in the references. Nevertheless, we hope that every work relevant to these lectures, however indirectly, will either be explicitly found in the bibliography at the end or at least in the reference lists of the referenced items. I apologize in advance for any shortcomings in this respect.

The audience of the lectures was composed predominantly of graduate students of universities across Italy and elsewhere in Europe, for that reason, the emphasis is not so much in rigor but in creating an understanding of the subject, good enough to be aware of its manifold applications. There are several very good general references, the most accesible to students is, in my view, [He1]. For deeper analysis of the Radon transform the reader is suggested to look in [He2] and [He3]. For a very clear explanation of the numerical algorithms of the (codimension one) Radon transform in $\mathbf{R}^2$ and $\mathbf{R}^3$, see [Na] and [KS]. There have also been many recent conferences on the subject of these lectures, for a glimpse into them we suggest [GG] and [GM].

Finally, I would like to thank the organizers, Enrico Casadio Tarabusi, Massimo Picardello, and Giuseppe Zampieri, for their kindness in inviting me and for the effort they exerted on the organization of this CIME session. I am also grateful to David Walnut for suggestions that improved noticeably these notes.

1. Tomographic imaging of space plasma

[1]These lectures reflect research of the author partially supported by the National Science Foundation.

Space plasma is composed of electrically charged particles that are not uniformly distributed in space and are influenced by celestial bodies. The problem consists in determining the distribution function of the energy of these particles (or of their velocities) in a region of space. A typical measuring device will take discrete measurements (for instance, sample temperatures at different points in space) and then the astrophysicist will try to fit a "physically meaningful" function passing through these points. The procedure proposed in [ZCMB] is based on the idea that the measurements should directly determine the distribution function. We do it by exploiting the charged nature of the particles and using the Radon transform. (The recently launched Wind satellite carries a measuring device based on similar interaction principles and requires tomographic ideas for the processing of the data.)

The advantage of the tomographic principles that we shall describe presently is that each measurement carries global information and seems to have certain noise reduction advantages over the pointwise measurements of temperatures, which is the usual technology. We will describe everything in a two-dimensional setting, but the more realistic three-dimensional case can be handled similarly.

The instrument we proposed in [ZCMB] is schematically the following. An electron enters into the instrument (a rectangular box in the figure below) through an opening located at the origin and is deflected by a constant magnetic field $\vec{B}$ perpendicular to the plane of the paper (see Figure 1). Under the Lorentz force, the electrons follow circular orbits and strike detectors located on the front-inside surface of the box (along the y axis). Those that strike a detector located at the point y have the property that

$$y = (2m/eB)v_x$$

where m is the mass of the electron, e its charge, and B the magnitude of the magnetic field $\vec{B}$. In other words, all the electrons with the same first component v_x of their velocities strike the same detector located at the height y. The range of velocities over a segment of width a (width of the detector) is

$$\Delta v_x = (eB/2m)d$$

(In terms of the length of the detector plate D in Figure 1 and the maximum velocity $v_{\max}$ we have $\Delta v_x = (d/D)\cdot v_{\max}$). If $f(v_x, v_y)$ represents the electron

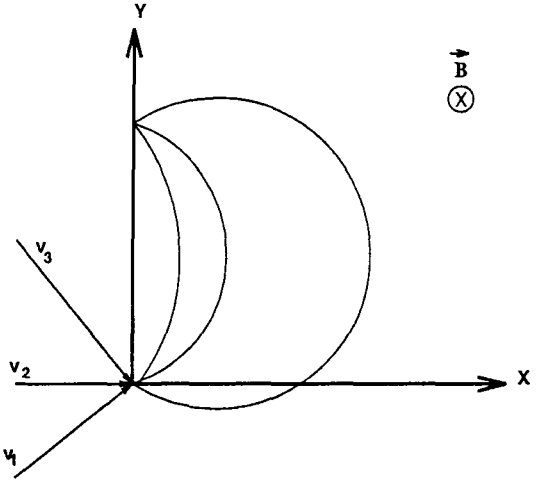

Figure 1: Schematic detector.

velocity distribution, then the number dN of electrons counted by a detector in time dt is given by

$$dN = An_e v_x \Delta v_x \int_{-\infty}^{\infty} f(v_x, v_y) dv_y \cdot dt,$$

n_e is electron density and A is the area of the entrance aperture. In other words,

$$\int_{-\infty}^{\infty} f(v_x, v_y) dv_y = \frac{1}{An_e \Delta v_x} \frac{dN}{dt}$$

so that the count of hits provides the integral of f along a line $v_x =$ constant in the velocity plane. By rotating the detector or changing the orientation of the magnetic field we obtain the Radon transform of f.

As a realistic example, consider a plasma of nominal electron density $n_e = 10\ cm^{-3}$, velocity in the range $v_{\min}$ to $v_{\max}$ of 1.2×10^8 to $3.0\times10^9\ cm\ s^{-1}$, average velocity $\bar{v} = 6.5\times10^8\ cm\ s^{-1}$, and we assume a Gaussian distribution function

$$f(v_x, v_y) = \left(\frac{1}{\sqrt{2\pi}\bar{v}}\right)^2 \exp\left(-\frac{(v_x - \bar{v})^2 + (v_y - \bar{v})^2}{2\bar{v}^2}\right)$$

so that

$$\frac{dN}{dt} = \text{ const. } \exp\left(-\frac{v_x^2}{2\bar{v}^2}\right)$$

with individual detector area and aperture of 0.04 cm^2 for a small instrument one gets that the distribution function f varies from 1 to 10^{-5} while dN/dt varies from 10^2 to $10^6 s^{-1}$. The standard measurement methods make the a priori assumption that f is the sum of a Gaussian centered at $\bar{v}$ and perturbed by adding a finite collection of Gaussians, often located in the region where f varies from 10^{-4} to 10^{-5}, but the previously described instrument does not require any such assumption, on the other hand, experimentally one sees that such large variations, like from 1 to 10^{-5} as in the example, are realistic. We shall see in Section 2 that this is an embodiment of the Radon transform in $\mathbf{R}^2$. The more realistic case of 3-d is handled by an instrument where there is a plane which contains the entrance aperture and a 2-d array of detectors in the plane (x, y). One shows that at each detector location (x, y) one obtains an integral over a planar curve and that the addition of overall elements with the same x component leads to a 2-d plane integral of the density distribution so that we have the Radon transform in $\mathbf{R}^3$. (This is an observation we made jointly with M. Shahshahani.)

Before concluding this section, let us remark that the large variations expected from the velocity density function f make the inversion of the Radon transform very ill-conditioned, even if f is assumed to be a smooth function. This is due to the continuity properties of the Radon transform and its inverse as seen in the next section. The remarkable point is that in medical applications, like CAT scans, the unknown density is naturally discontinuous along some curves but otherwise it has small local variations, and it is this reason the inversion problem is ultimately easier for medical applications.

2. The Radon Transform in $\mathbf{R}^2$

Let $\omega \in S^1, \omega = (\cos\theta, \sin\theta)$, and take $p \in \mathbf{R}$. The equation $x \cdot \omega = p$ represents the line l which has (signed) distance p from origin and is perpendicular to the direction ω.

For any reasonable function f (e.g., continuous of compact support), we can compute the line integral, with respect to Euclidean arc length ds,

$$Rf(\omega, p) := \int_{x \cdot \omega = p} f(x) ds = \int_{-\infty}^{\infty} f(x_0 + t\omega^{\perp}) dt \tag{1}$$

where x_0 is a fixed point in l, i.e., satisfying the equation $x_0 \cdot \omega = p$, and $\omega^{\perp} = (-\sin\theta, \cos\theta)$ is the rotate of ω by $\pi/2$.

The map $f \mapsto Rf$ is called the Radon transform and Rf is called the Radon transform of f. Clearly Rf is a function defined on $S^1 \times \mathbf{R}$ (that is, the family of all lines in $\mathbf{R}^2$) with the obvious compatibility condition:

$$(Rf)(-\omega, -p) = Rf(\omega, p). \tag{2}$$

There are several reasonable domains of definition for R such as $L^1(\mathbf{R}^2), \mathcal{S}(\mathbf{R}^2)$, etc., but in many applications it is enough to consider functions which are of compact support, with singularities which are only jumps along reasonable curves, and otherwise smooth. This is obviously the transformation appearing in Section 1. The full 3-d instrument there corresponds to integration over planes in $\mathbf{R}^3$, perpendicular to a unit vector ω. A big source of interest of this transform lies in CAT (Computerized Axial Tomography) as a radiological tool where each planar section of a patient is scanned by X-rays as in Figure 2.

In this particular case it can be seen that

$$\log \frac{I_0}{I} \approx \int_l \mu ds \tag{3}$$

where I_0 is the radiation intensity at the source and I is the intensity measured at the detector. The attenuation is a consequence of traversing a tissue of density μ. So the data collected from this X-ray scanning appears in the form of the Radon transform $R\mu$ of the density μ, computed for a finite collection of directions $\omega_1, \omega_2, \ldots, \omega_N$ (usually equally spaced) and a finite collection of lines, i.e., values $p_1, p_2, \ldots, p_M$ for each direction. This is called

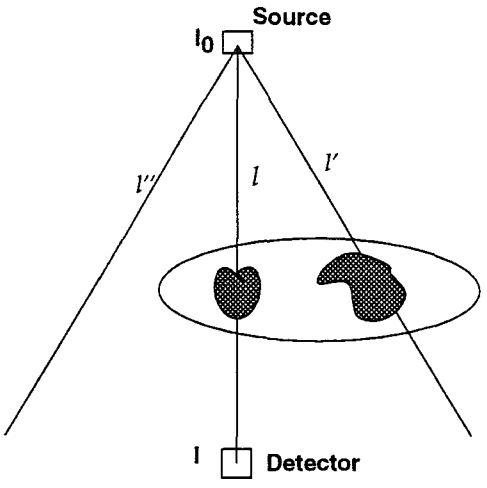

Figure 2: Schematic CAT scanner.

a "parallel beam" CT scanner. The configuration that it is now most used but we shall not discuss here is the "fan beam" CT scanner, we refer to [Na], [KS] for a discussion of the differences of these two cases, they really only appear at the implementation level of the inversion algorithms because only a limited amount of data can be obtained in the real world.

Some easy properties of the Radon transform are obtained by observing that Rf can be written using distributions. In fact, if we introduce the unit density $\delta(p - x \cdot \omega)$ which is supported by the line $x \cdot \omega = p$, then

$$Rf(\omega, p) = \int_{\mathbf{R}^2} f(x)\delta(p - x \cdot \omega)dx \tag{1'}$$

with the usual abuse of language.

It is also convenient to write

$$R_\omega f(p) = Rf(\omega, p). \tag{4}$$

Formula (1') can be used to extend Rf to $(\mathbf{R}^2 \setminus \{0\}) \times \mathbf{R}$, using the fact that $\delta(p - x \cdot \omega)$ is homogeneous of degree -1; indeed, one defines

$$Rf(\xi, s) = \frac{1}{|\xi|} Rf\left(\frac{\xi}{|\xi|}, \frac{s}{|\xi|}\right). \tag{5}$$

One can therefore take derivatives of (1′) with respect to the variables $\xi_j (\xi = (\xi_1, \xi_2))$ and obtain

$$\frac{\partial}{\partial \xi_j} Rf(\xi, s) = \int f(x) \frac{\partial}{\partial \xi_j} \delta(s - x \cdot \xi) dx \ (j = 1, 2), \tag{6}$$

but

$$\frac{\partial}{\partial \xi_j} \delta(s - x \cdot \xi) = -x_j \delta'(s - x \cdot \xi)$$

and

$$\frac{\partial}{\partial s} \delta(s - x \cdot \xi) = \delta'(s - x \cdot \xi)$$

so that

$$\begin{aligned} \frac{\partial}{\partial \xi_j} Rf(\xi, s) &= - \int f(x) x_j \delta'(s - x \cdot \xi) dx \\ &= - \frac{\partial}{\partial s} \int f(x) x_j \delta(s - x \cdot \xi) dx \\ &= - \frac{\partial}{\partial s} (R(x_j f)(\xi, s)). \end{aligned}$$

On the other hand the Radon transform of the derivative of f is:

$$\begin{aligned} R_\xi \left(\frac{\partial}{\partial x_j} f\right)(s) &= \int \frac{\partial f}{\partial x_j}(x) \delta(s - x \cdot \xi) dx \\ &= \xi_j \int f(x) \delta'(s - x \cdot \xi) dx \\ &= \xi_j \frac{\partial}{\partial s} (R_\xi f)(s). \end{aligned} \tag{7}$$

In particular, for

$$\Delta = \frac{\partial^2}{\partial \xi_1^2} + \frac{\partial^2}{\partial \xi_2^2},$$

one obtains

$$R_\xi(\Delta f)(s) = (\xi_1^2 + \xi_2^2)\frac{\partial^2}{\partial s^2}(R_\xi f)(s). \tag{7'}$$

When ξ is restricted to be an element $\omega \in S^2$, we get,

$$(R\Delta f)(\omega, s) = \frac{\partial^2}{\partial s^2} Rf(\omega, s); \tag{8}$$

In other words, R intertwines Δ and $\frac{\partial^2}{\partial s^2}$ when the arguments are restricted to $S^1 \times \mathbf{R}$. Another useful property is the following:

$$R_\omega(f * g) = R_\omega f \otimes R_\omega g, \tag{9}$$

where the symbol $*$ on the left side of (9) denotes the convolution in $\mathbf{R}^2$ and $\otimes$ denotes the convolution product in $\mathbf{R}$. The easiest way to verify (9) is via the Fourier Slice Theorem, which we recall here:

Let $\mathcal{F}_1$ denote the Fourier transform of a function in $\mathbf{R}$ and $\hat{f}$ or $\mathcal{F}_2$ the Fourier transform of a function f in $\mathbf{R}^2$. Then

$$\mathcal{F}_1(R_\omega f)(\tau) = \hat{f}(\tau\omega). \tag{10}$$

The proof is as follows,

$$\begin{aligned}
\mathcal{F}_1(R_\omega f)(\tau) &= \int_{-\infty}^{\infty} e^{-2\pi i t\tau} R_\omega f(t) dt \\
&= \int_{-\infty}^{\infty} e^{-2\pi i t\tau} \left[\int_{-\infty}^{\infty} f(t\omega + s\omega^\perp) ds \right] dt \\
&= \int_{\mathbf{R}^2} e^{-2\pi i t\tau} f(t\omega + s\omega^\perp) ds dt,
\end{aligned}$$

Letting now $x = t\omega + s\omega^\perp$, one has $t = x \cdot \omega$ and $dtds = dx$, the Lebesgue measure in $\mathbf{R}^2$, in the previous equation we obtain

$$\begin{aligned}\mathcal{F}_1(R_\omega f)(\tau) &= \int_{\mathbf{R}^2} e^{-2\pi i(x\cdot\omega)\tau} f(x)dx \\ &= \hat{f}(\tau\omega).\end{aligned}$$

■

Recalling that in $\mathbf{R}^2$

$$\mathcal{F}_2(f * g)(\xi) = \hat{f}(\xi)\hat{g}(\xi),$$

we can easily prove (9). Indeed, from (10) we have

$$\begin{aligned}\mathcal{F}_1(R_\omega(f * g))(\tau) &= \mathcal{F}_2(f * g)(\tau\omega) = \hat{f}(\tau\omega)\hat{g}(\tau\omega) \\ &= \mathcal{F}_1(R_\omega f)(\tau)\mathcal{F}_1(R_\omega g)(\tau) = \mathcal{F}_1(R_\omega f \otimes R_\omega g)(\tau)\end{aligned}$$

and therefore, by the injectivity of $\mathcal{F}_1$, we get $R_\omega(f * g) = R_\omega f \otimes R_\omega g$.

Let us also note that if τ_a denotes the translation by a, i.e., $\tau_a f(x) = f(x-a)$, then

$$R(\tau_a f)(\omega, p) = R[f(x-a)](\omega, p) = R_\omega f(p - \omega \cdot a) = \tau_{\omega\cdot a} Rf(p).$$

We now proceed to state some inversion formulas, which give different ways to recover f from Rf.

Fourier Inversion Formula:

$$f(x) = \int_0^\infty \tau d\tau \int_{S^1} e^{i2\pi\tau x\cdot\omega} \mathcal{F}_1(R_\omega f)(\tau)d\omega \tag{11}$$

The proof is clear, we begin with the Inversion Theorem for the Fourier transform. We have

$$f(x) = \int_{\mathbf{R}^2} e^{2\pi i x\cdot\xi} \hat{f}(\xi)d\xi,$$

let $\xi = \tau\omega$ and integrate in polar coordinates, to obtain

$$f(x) = \int_0^\infty \tau d\tau \int_{\omega \in S^1} e^{2\pi i \tau x \cdot \omega} \hat{f}(\tau\omega) d\omega.$$

We now apply the Fourier Slice Theorem to get

$$f(x) = \int_0^\infty \tau d\tau \int_{\omega \in S^1} e^{2\pi i \tau x \cdot \omega} \mathcal{F}_1(R_\omega f)(\tau) d\omega.$$

■

This inversion formula can be implemented numerically using the Fast Fourier Transform (FFT) (see [Na]). Quite often the points $\tau\omega$ where the data $\mathcal{F}_1(R_\omega f)(\tau)$ is known do not have a lattice structure. This causes problems for the FFT but we can use rebinning algorithms like [ST] to obviate this problem.

To obtain another kind of inversion formula we observe the following:

$$\int_{-\infty}^{\infty} R_\omega f(s) g(s) ds = \int_{-\infty}^{\infty} \int_{-\infty}^{\infty} f(s\omega + t\omega^\perp) g(s) dt ds,$$

Let $x = s\omega + t\omega^\perp$ so that $s = x \cdot \omega, dx = dtds$, and therefore

$$\int_{-\infty}^{\infty} R_\omega f(s) g(s) ds = \int_{\mathbf{R}^2} f(x) g(x \cdot \omega) dx$$

i.e., the adjoint of R_ω is the operator $R_\omega^\#$ defined by

$$R_\omega^\# g(x) = g(x \cdot \omega). \tag{12}$$

We now consider for an arbitrary function $g(\omega, s)$, having the symmetry $g(-\omega, -s) = g(\omega, s)$,

$$\int_{S^1 \times \mathbf{R}} Rf(\omega, s) g(\omega, s) d\omega ds = \int_{S^1} d\omega \int_{-\infty}^{\infty} R_\omega f(s) g(\omega, s) ds$$

$$= \int_{S^1} d\omega \int_{-\infty}^{\infty} f(s\omega + t\omega^\perp) g(\omega, s) ds dt$$

(with the usual substitution, $x = s\omega + t\omega^{\perp}$, etc., we get)

$$\begin{aligned} &= \int_{S_1} d\omega \int_{\mathbf{R}^2} f(x) g(\omega, \omega \cdot x) d_2 x \\ &= \int_{\mathbf{R}^2} f(x) \left[\int_{S^1} g(\omega, \omega \cdot x) d\omega \right] d_2 x \\ &= \int_{\mathbf{R}^2} f(x) \left[\int_{S^1} R_{\omega}^{\#} g(x) d\omega \right] d_2 x \\ &= \int_{\mathbf{R}^2} f(x) R^{\#} g(x) d_2 x. \end{aligned} \tag{13}$$

The operator $R^{\#}$ defined by (13) is known by the name of "backprojection operator". Note, in this regard, that $g(\omega, s)$ is a function of "lines" and that $R^{\#}g(x)$ is its integral over all lines passing through x. It is easy to prove the following useful property of the backprojection operator

$$(R^{\#}g) * f = R^{\#}(g \otimes Rf), \tag{14}$$

where the convolution $\otimes$ in the second member clearly takes place in the second variable. This identity plays an important role in the numerical inversion of the Radon transform.

Finally, we get to the following important result:

$$R^{\#}Rf = \frac{2}{|x|} * f. \tag{15}$$

Indeed,

$$\begin{aligned} R^{\#}Rf(x) &= \int_{S^1} Rf(\omega, \omega \cdot x) d\omega \\ &= \int_{S^1} d\omega \int_{-\infty}^{\infty} f((\omega \cdot x)\omega + s\omega^{\perp}) ds \\ &= \int_{S^1} d\omega \int_{-\infty}^{\infty} f(x + s\omega^{\perp}) ds \end{aligned}$$

$$= 2 \int_{S^1} d\omega \int_0^\infty f(x + s\omega^\perp) ds$$

By setting $y = s\omega^\perp, s = |y|, dy = sd\omega ds$ we get

$$\begin{aligned} R^\# Rf(x) &= 2 \int_{\mathbf{R}^2} \frac{1}{|y|} f(x+y) dy \\ &= 2 \int_{\mathbf{R}^2} \frac{1}{|x-y|} f(y) dy, \end{aligned}$$

which is exactly (15). Since one has $\mathcal{F}_2 \frac{1}{|y|} = \frac{1}{|\xi|}$ (see e.g. [He2, page 134]), one deduces that

$$\mathcal{F}_2(R^\# Rf)(\xi) = \frac{2}{|\xi|} \hat{f}(\xi).$$

One can therefore conclude that the inversion operator Λ is such that

$$\hat{\Lambda}(\xi) = \frac{|\xi|}{2}$$

so that

$$f(x) = \frac{1}{2} \int_{\mathbf{R}^2} e^{2\pi i x \cdot \xi} |\xi| \widehat{(R^\# Rf)}(\xi) d\xi = \Lambda R^\# Rf(x), \tag{16}$$

which is sometimes called the backprojection inversion formula.

Reorganizing the terms in the last formula one can rewrite it to obtain a more standard form, where the filtering is one dimensional.

Filtered backprojection inversion formula:

$$f = \frac{1}{4\pi} R^\# H(Rf)' \tag{17}$$

where

$$(Rf)'(\omega, s) = (\frac{\partial}{\partial s} R_\omega f)(s)$$

and H is the Hilbert transform defined by

$$Hg(s) = \frac{1}{\pi} \int_{-\infty}^{\infty} \frac{g(t)}{s-t} dt,$$

where the last integral is understood in the sense of principal value. In other words,

$$f(x) = \frac{1}{(2\pi)^2} \int_{S^1} \int_{\mathbf{R}} \frac{(Rf)'(\theta, t)}{x \cdot \theta - t} dt d\theta. \tag{18}$$

No introduction to the Radon inversion formula can be complete without at least mentioning the inversion formula due to Radon, which among other things, is akin to the inversion formula for the hyperbolic Radon transform due to Helgason, which will be mentioned below. Consider for a fixed $x \in \mathbf{R}^2$, the average of Rf over all lines at a distance $q \geq 0$ from x, namely, let

$$F_x(q) := \frac{1}{2\pi} \int_{S^1} Rf(\omega, \omega \cdot x + q) d\omega.$$

Radon found that

$$f(x) = -\frac{1}{\pi} \int_0^{\infty} \frac{dF_x(q)}{q}. \tag{19}$$

We refer to [GM] for the original 1917 paper and commentaries.

An approximate implementation of (17) can be given by using the Fourier inversion formula

$$f(x) \approx \int_0^{\pi} Q_\theta(x \cdot \omega) d\theta \tag{20}$$

where, as above, $\omega = (\cos\theta, \sin\theta)$ and

$$\begin{aligned} Q(t) &= \int_{-b}^{b} |\tau| e^{2\pi i t\tau} \mathcal{F}_1(Rf)(\tau) d\tau \\ &\approx \int_{-\infty}^{\infty} |\tau| e^{2\pi i t\tau} \mathcal{F}_1(Rf)(\tau) d\tau. \end{aligned}$$

This last approximation constitutes a band limiting process, and it can also be obtained from (14) as follows: Let w_b be a "band-limiter", i.e, $supp(\omega_b) \subseteq [-b, b]$ and $W_b = R^{\#} w_b$. Then (by letting $g = w_b$ in (14)), we obtain

$$W_b * f = R^{\#}(w_b \otimes Rf)$$

that is, we want W_b to be an approximate δ-function (cf. [Na, Ch. 5]). To begin with, choose W_b radial, e.g.,

$$\hat{W}_b(\xi) = \frac{1}{2\pi}\hat{\Phi}(\frac{|\xi|}{b})$$

where $0 \leq \hat{\Phi}(\sigma) \leq 1, \hat{\Phi} = 0$ for $\sigma \geq 1$; this implies that $w_b =$ const. $|\sigma|\hat{\Phi}(\frac{|\sigma|}{b})$. The previous example is given by the ideal lowpass filter defined by

$$\hat{\Phi} = \begin{cases} 1 & \text{if } 0 \leq \sigma < 1 \\ 0 & \text{if } \sigma \geq 1 \end{cases}$$

and so

$$W_b(x) = \frac{1}{2\pi} b^2 \frac{J_1(b|x|)}{(b|x|)},$$

where J_1 is the Bessel function of the first kind and order one.

We shall see below that one of the wavelet-based inversion formulas is inspired by (20).

The formulas (15), (16), (17) allow for rather precise estimates of the degree in which the Radon transform and its inverse preserve the smoothness of the function f and data Rf. One way to measure this is to do it using Sobolev norms defined in an obvious way in the space of functions in the space of all lines. For instance, if $f \in C_0^\infty(B)$, where B is the unit disk in $\mathbf{R}^2$, then one can find in [Na, Theorem 3.1], that for any real α, there are constants $c, C > 0$ such that

$$c||f||_{H_0^\alpha(B)} \leq ||Rf||_{H^{\alpha+1/2}} \leq C||f||_{H_0^\alpha(B)} \tag{21}$$

In the particular case of $\alpha = 0$, we see that for $f \in L_0^2(\mathbf{R}^2)$ and $supp(f) \subset\subset B$ one cannot expect better than control of one-half derivatives of Rf.

Useful variations of the estimates (21) for *other* kinds of Radon transform can be found using that $R^{\#}R$ is a Fourier integral operator of elliptic type [GS].

3. Localization of the Radon transform

Returning to the problem of plasma physics that started these lectures, besides the fact that the functions we are trying to detect seem to have a very large variation, that is, a large H^1 norm, we have the added difficulty that the amount of data one can process or send down to Earth is fairly limited. One knows experimentally that, on a first approximation, all the variations from being Gaussian occur in the region where the values of f have gone down by 4–5 orders of magnitude. That is, if f has a value 1 for the bulk velocity, then we are interested in the region where the values of f lie between 10^{-4} to 10^{-5}. The way this problem was traditionally solved (for conventional measuring devices) was to assume f had the form of a linear combination of a small number of Gaussians, and one just tries to estimate the variances and coefficients of these perturbation terms. If one does not want to impose these a priori restrictions on f, and we have only limited amount of data to use, a natural idea is to just use those lines that cross only the annular region where the main Gaussian varies between 10^{-4} and 10^{-5}. (In the case of dimension 3 we would be dealing with a shell instead of an annulus.) This requires a *localization* of the Radon Transform. There are two ways to proceed. One, the most obvious (*or naive*) way is to try to localize the Radon transform as follows:

Reconstruct a function f in a disk $B(a,r)$ from the data $Rf(\ell)$, using only lines ℓ passing through $B(a,r)$.

This cannot be true in dimension 2, as observed already by F. John. The reason is the well-known fact that waves cannot be localized in 2-dimensions, namely, if we drop a pebble in the water, the ripples propagate along ever-expanding disks with time. In other words, an arbitrary perturbation confined to a disk at time $t = 0$ does not necessarily remain confined to the same disk (or any concentric disk, for that matter) at all future times. On the other hand, as F. John pointed out [J], if u is a solution of the wave equation $\Delta u - u_{tt} = 0$, then its Radon transform $v = Ru$ is a solution of the one dimensional wave equation $v_{ss} - v_{tt} = 0$, as it is seen immediately from the relation (8). For the one-dimensional wave equation with initial conditions at time $t = 0, v(s,0) = v_0(s)$ and $\frac{\partial}{\partial t}v(s,0) = v_1(s)$, we have

$$v(s,t) = \frac{1}{2}(v_0(s-t) + v_0(s+t)) + \frac{1}{2}\int_{s-t}^{s+t} v_1(\tau)d\tau.$$

If we think the pebble as being given by $u(x,0) = u_0(s) = 0$ for $|x| \geq \epsilon, 0 < \epsilon << 1$, and $u_t(x,0) = u_1(x) \equiv 0$, then for a fixed $\omega \in S^1$ and any later time $t > 0$ we would have with $v(s,t) = R(u(\cdot,t))(\omega,s)$ that $v_0(s) = v(s,0) = 0$ for $|s| \geq \epsilon$ while $v_1(s) = v_t(s,0) \equiv 0$. Thus, at any later time $t > \epsilon$ we have that $v(s,t)$ is only different from 0 for $t - \epsilon \leq |s| \leq t + \epsilon$. Thus, the strict localization of the Radon transform would impose that the support of $u(x,t)$ be in the annulus $t - \epsilon \leq |x| \leq t + \epsilon$, which contradicts our observations. (Nevertheless, we shall see that some sort of localization takes place.)

The other alternative, which fits the plasma problem, is to try to see whether we could reconstruct the values of f outside of a disk from the values of $Rf(\ell)$, with ℓ never crossing that disk. This turns out to be possible! It is the *exterior problem* for the Radon transform. We follow here the work of Quinto [Q1], [Q2] (and references therein.)

The starting point, as recognized in the pioneering work of A. M. Cormack, is to expand both the function f and its Radon transform $g = Rf$ in a Fourier series. (For $\mathbf{R}^n, n > 2$, one uses spherical harmonics [Na, p. 25 ff.]) That is,

$$\begin{aligned} f(x) &= \sum_{\ell=-\infty}^{\infty} f_\ell(r) e^{i\ell\theta} \quad x = (r\cos\theta, r\sin\theta), \\ g(\omega,s) &= \sum_{\ell=-\infty}^{\infty} g_\ell(s) e^{i\ell\theta} \quad \omega = (\cos\theta, \sin\theta). \end{aligned}$$

Then, the Fourier coefficients f_ℓ and g_ℓ are related by the two formulas

$$g_\ell(s) = 2\int_s^\infty T_{|\ell|}(\frac{s}{r})(1 - \frac{s^2}{r^2})^{-1/2} f_\ell(r)dr, \tag{22}$$

$$f_\ell(r) = -\frac{1}{\pi}\int_r^\infty T_{|\ell|}(\frac{s}{r})(s^2 - r^2)^{-1/2} g'_\ell(s)ds, \tag{23}$$

where T_ℓ is the Chebyshev polynomial of the first kind. One of the consequences of the Fourier Slice Theorem is that g cannot be an arbitrary function in the space of lines, it must satisfy certain compatibility conditions, usually called the moment conditions,

$$\int_{-\infty}^{\infty} s^{m-1} g(\omega, s) ds \in \text{ span}\{e^{ik\theta}, |k| < m\}, \ \omega = e^{i\theta}.$$

This allows for a modification of (23) that makes it far more practical for numerical purposes [Na, p. 29-30]. This pair of equations show that the values of $Rf(\ell)$ over all lines *exterior* to the disk $B(0,r)$ are thought to determine f in the exterior of $B(0,r)$. In particular, if one has

$$\text{supp } f \subseteq B(0, \rho_0),$$

then the values of f in the annulus $\rho_1 < |x| < \rho_0$ are entirely determined by the measurements of the $Rf(\ell)$, only for lines ℓ that intersect this annulus. (The uniqueness of the exterior problem and its variants is usually called the support theorem. It was first proved by Helgason in 1965, we refer to [He1], [He2] for details and generalizations.)

Quinto [Q1], [Q2] has successfully used this kind of ideas to obtain a very effective tomographic algorithm to determine cracks in the exterior shell of (usually large) circular objects, for instance, rocket nozzles. The method of Quinto is based on two things. First, the known characterization of the kernel of the exterior Radon transform in L^2 spaces with convenient radial weights (this is due to Perry for $n = 2$ and Quinto for $n \geq 3$). For the case of interest at hand, $n = 2$, we consider the kernel of the exterior Radon transform in $L^2(B_1^c, r dx)$, then the Fourier coefficients $f_\ell(r)$ must be given by the rule

$$f_\ell(r) = \text{ linear combination of } r^{2-k}, 0 \leq k \leq |\ell|, |\ell| - k \text{ even.} \qquad (24)$$

For instance,

$$f_0 = 0, f_1 = 0, f_2 = cr^{-2}, f_3 = cr^{-3}, f_4 = c_1 r^{-2} + c_2 r^{-4}, \ldots$$

The second observation is the fact that the Radon transform maps $H_1 := L^2(B_1^c, r(1-r)^{1/2} dx)$ into $H_2 = L^2(S^1 \times (1, \infty), \frac{dwds}{s})$ and one has an explicit diagonalization procedure for R, so that there are orthonormal bases φ_j and ψ_j, respectively of $H_1 \ominus \ker R$ and of $ImR \subseteq H_2$, so that

$$R\varphi_j = \kappa_j \psi_j \quad \text{with } \kappa_j > 0$$

and κ_j explicitly computable. Thus, for a given f of $L^2_c(B^c_1, dx)$ (i.e., of compact support), we have

$$f = \sum_{j=1}^{\infty} a_j \varphi_j + \tilde{f} \quad \text{with } \tilde{f} \in \ker R \cap L^2_c(B^c_1, dx)$$

so that

$$Rf = \sum_{j=1}^{\infty} a_j \kappa_j \psi_j$$

thus

$$a_j = \frac{1}{\kappa_j} < Rf, \psi_j >_{H_2}$$

This determines exactly $\tilde{g} = f - \tilde{f}$. One expands now $\tilde{f}$ in a Fourier series $\sum f_\ell(r) e^{i\ell\theta}$, with f_ℓ of the form (22) as mentioned earlier. Now for $r >> 1$ we know that $f \equiv 0$, so that $\tilde{f} = -\tilde{g}$, thus, for $r >> 1$ we have $f_\ell(r) = -\int_{-\pi}^{\pi} e^{-i\ell\theta} \tilde{g}(re^{i\theta}) d\theta$, but the coefficients $f_\ell(r)$ are polynomials in $1/r$, so they are completely determined everywhere (up to $r = 1$) by their values for $r >> 1$. It is here that one uses a sort of analytic continuation, so it is fairly unstable, but Quinto has modified further this algorithm if one assumes f to be known in the small annulus $1 \leq |x| \leq 1 + \epsilon$, to give it further stability [Q2].

In the context of the plasma problem, we compared numerically the use of the same number of data measurements $Rf(\ell)$, either spread throughout the whole disk versus the measurements taken only (and thus more densely) in the annulus of interest. We found the surprising result (to us) that the standard algorithm, with more thinly spread measurements did better. It was this numerical observation that led to the search of a different way to localize the Radon transform using wavelets.

Let us first review briefly two other localization methods that had appeared earlier in the literature.

The first one is the following. Let us assume that the unknown function f has support in the disk B_1 of center 0 and radius 1, but that we are only interested on the values of f in $B_b, 0 < b < 1$, while we collect data on $B_a, 0 < b \leq a \leq 1$. (Note that all the disks are centered at 0). This is

the situation considered for the *interior* Radon transform [Na, VI.4]. The basic idea is to make $Rf(\ell) = 0$ when ℓ doesn't intersect B_a and apply the standard reconstruction algorithm. In other words, we want to obtain (even approximately) the values $f(x), |x| \leq b$, from $R(f\chi_a)$, where χ_a stands for the characteristic function of the disk B_a. The first problem is that there are many non-zero functions f that have $R(f\chi_a) = 0$. Luckily, these functions do not vary much on B_b [Na], so one could just try to find f *up to an additive constant* (and try to find that constant by other means). One can see from the table or the formula (4.4) in [Na, p. 170], that one needs $a = 4b$ to obtain a maximum L^∞ error of 1.6% of the L^2 norm of f in B_1. In particular, this procedure could not be applied if we are interested in $f(x)$, for $x \in B(x_0, a) \subseteq B_1$ with x_0 close to ∂B_1. A typical such example is that of spinal chord studies. Usually, one study involves 40-60 CAT scans, that is, 40-60 scans along body sections perpendicular to the spine at different heights. The spinal chord area is about 15% of any such cross section of the body, and there would be a substantial reduction of radiation received by the patient if one localizes the CAT scan to only those lines passing through or near the spinal chord area.

Another alternative that has been proposed is that of Λ-tomography [FRK], where one only attempts to reconstruct to discontinuities of the function f, i.e., perform edge detection in the image. The principle is based on the formula (15) namely, consider the "approximate" inversion

$$\tilde{f} = \Delta R^{\#} Rf,$$

so that $\tilde{f} = 4\pi\Lambda f$. This formula preserves the "edges" (= discontinuities of f) but not the actual values of f. A variation of this formula has been implemented in the Mayo Clinic to study angiograms [FRK].

Another interesting consequence of this kind of approximate formula is that it can also be applied to the *attenuated* Radon transform,

$$R_\mu f(w, s) = \int_{-\infty}^{\infty} f(sw + tw^\perp)\mu(sw + tw^\perp, w)dt$$

where $\mu(x, w)$ is assumed to be real analytic in $\mathbf{R}^2 \times S^1$ and nonnegative. This appears in SPECT tomography and, usually, both f and μ are unknonwn. As observed by Kuchment and collaborators [KLM] the function $\Delta R^{\#} R_\mu f$

will have the same singularities as f. The point is that $R^{\#}R_{\mu}$ is still an elliptic Fourier integral operator. This fact had already been used effectively by many people, most notably Boman and Quinto [BQ], and it is the key observation in the work of Quinto [Q3], Ramm and Zaslavsky [RZ], and others.

The method of localization we want to discuss here with a bit more detail is that of using wavelets to invert and localize the Radon transform in dimension 2. This general principle, which is joint work with David Walnut, was presented first in a 1990 NATO conference [W], and independently in [Ho]. Since then, similar ideas have appeared elsewhere in the literature (see, for instance, the recent volume [AU], the papers [BW1], [BW2], [DB], [DO], [O], and references therein.) True localization using discrete wavelets and filter banks is clearly developed in [FLBW]. (See also [FLB] for the fan beam case.)

There are many excellent books on the subject of wavelets, at all levels of sophistication and different points of view, the following is a very partial list [M], [D], [Ka]. There are actually two different, albeit related concepts, the *continuous wavelet transform* (CWT) (easier to understand) and the *discrete wavelet transform* (DWT) (easier to work with).

The idea of CWT originates from the standard properties of the Fourier transform representation of nice functions. For $f \in L^2(\mathbf{R})$ or $f \in \mathcal{S}(\mathbf{R})$, we have both

$$\begin{aligned} \hat{f}(\xi) &= \int_{-\infty}^{\infty} f(x)e^{-2\pi ix\xi}dx \\ f(x) &= \int_{-\infty}^{\infty} \hat{f}(\xi)e^{2\pi ix\xi}d\xi \end{aligned}$$

and

$$||\hat{f}||_2 = ||f||_2 = (\int_{-\infty}^{\infty} |f(x)|^2 dx)^{1/2}$$

If we translate f by $b \in \mathbf{R}, \tau_b f(x) := f(x-b)$, then $(\tau_b f)\hat{}(\xi) = e^{2\pi ib\xi}\hat{f}(\xi)$, and for dilations we have $D_a f(x) := \frac{1}{\sqrt{a}} f(x/a)(a > 0)$, so that $||f||_2 = ||D_a f||_2$ and

$$(D_a f)\hat{}(\xi) = D_{(1/a)}\hat{f}(\xi).$$

In other words, the group $x \to ax + b$ $(a > 0, b \in \mathbf{R})$ operates via unitary operators in $L^2(\mathbf{R})$, and has a corresponding representation on the space of Fourier transforms (which happens to coincide with $L^2(\mathbf{R})$). The "problem" of the Fourier transform representation is that the behavior of $\hat{f}$ at a point ξ depends on the values of f everywhere, for that reason, the idea of a "windowed" Fourier transform has been introduced long ago, namely, introduce a cut-off function g (say, a "smooth" approximation of $\chi_{[-1,1]}$) and consider

$$\mathcal{F}_1((\tau_b g)f)(\xi) = \int_{-\infty}^{\infty} g(x-b)f(x)e^{-2\pi i x\xi}dx.$$

Note that $\mathcal{F}_1((\tau_b g)f)(\xi)$ is $\check{\psi} * f(\xi)$, where ψ is the *wavelet* $\psi(x) = g(x)e^{2\pi i x\xi}$,$\check{\psi}(x) = \psi(-x)$. If we want to consider also the behavior at f at different scales we are led naturally to the CWT: Given a wavelet $\psi \in L^2(\mathbf{R})$, and $f \in L^2(\mathbf{R})$ we define

$$W_\psi f(a,b) := \int_{-\infty}^{\infty} f(t)\bar{\psi}(\frac{t-b}{a})\frac{dt}{\sqrt{a}} =< f, D_a\tau_b\psi >= (f * \overline{D_a\check{\psi}})(b) \qquad (25)$$

for $0 < a < \infty, b \in \mathbf{R}, \bar{\psi}$ denotes the complex conjugate of ψ, and $<,>$ denotes the L^2-scalar product. We assume the wavelet is "oscillatory", that is, it is an arbitrary function in $L^2(\mathbf{R})$ which satisfies the condition

$$c_\psi := \int_{-\infty}^{\infty} \frac{|\hat{\psi}(\xi)|^2}{|\xi|}d\xi < \infty.$$

This condition implies that $\int_{-\infty}^{\infty} \psi(x)dx = 0$. (For instance, when $\hat{\psi}$ is continuous at $\xi = 0$, which occurs if $\psi \in L^1(\mathbf{R}) \cap L^2(\mathbf{R})$.) In fact, later on we will be interested in wavelets with many vanishing moments

$$\int_{-\infty}^{\infty} x^k\psi(x)dx = 0, \quad 0 \le k \le N.$$

A typical wavelet is the Haar wavelet

$$\psi = \chi_{[0,1/2]} - \chi_{[1/2,1]}$$

so that

$$D_{1/2}\psi = \sqrt{2}(\chi_{[0,1/4]} - \chi_{[1/4,1/2]})$$

which shows that for $k \to \infty, D_{2^{-k}}\psi$ "analyzes" smaller and smaller details of the "signal" f.

Moreover, $W_\psi f$ determines f as seen from the following relation valid for any pair $f, g \in L^2(\mathbf{R})$

$$\int_{-\infty}^{\infty}\int_{-\infty}^{\infty} W_\psi f(a,b)\overline{W_\psi g(a,b)}\frac{dadb}{a^2} = c_\psi < f, g > ||\psi||_2^2,$$

usually called Calderon's identity. If $||\psi||_2 = 1$ one also has the L^2-approximation property

$$||f - \frac{1}{c_\psi}\int_{\substack{A_1 \le |a| \le A_2 \\ |b| \le B}} W_\psi f(a,b) D_a \tau_b \psi \frac{dadb}{a^2}|| \to 0 \qquad (26)$$

as $A_2 \to 0^+, A_2 \to +\infty, B \to +\infty$.

The generalization to $\mathbf{R}^n$ is easy. A function $\psi \in L^2(\mathbf{R}^n)$ is a wavelet if

$$\int_{\mathbf{R}^n} \frac{|\hat{\psi}(\xi)|^2}{|\xi|} d\xi < \infty$$

For a radial wavelet $\psi \in L^2(\mathbf{R}^n)$ and $f \in L^2(\mathbf{R}^n)$ we define the CWT by

$$W_\psi f(a,b) = f * D_2\bar{\psi}^\vee(b) \quad \text{for } a \in \mathbf{R} \setminus \{0\}, b \in \mathbf{R}^n,$$

where this time, $D_a\psi(x) = |a|^{-n/2}\psi(x/a)$.

The interest of the CWT for tomograpy lies in the following two propositions from [BW2].

Proposition 1. Let $\rho \in L^2(\mathbf{R})$ be real valued, even, and satisfying

$$\int_0^\infty \frac{|\hat{\rho}(r)|^2}{r^3} dr < \infty \tag{27}$$

Define a radial function ψ in $\mathbf{R}^2$ by $\mathcal{F}_2\psi(\xi) = 2\hat{\rho}(|\xi|)/|\xi|$, then ψ is a wavelet and

$$W_\psi f(a,b) = a^{-1/2} \int_{S^1} (W_\rho R_\omega f)(a, b \cdot \omega) d\omega \tag{28}$$

Proof. Using the Fourier Slice Theorem we have for $\gamma \in \mathbf{R}$

$$\frac{|\gamma|}{2} \mathcal{F}_1(R_\omega \psi)(\gamma) = \frac{|\gamma|}{2} (\mathcal{F}_2 \psi)(\gamma\omega) = \hat{\rho}(|\gamma\omega|). \tag{29}$$

It is then easy to verify that (27) implies that ψ is a wavelet in $\mathbf{R}^2$.

Recall that the Riesz transform of order α, $I^\alpha \varphi$, of a function $\varphi \in \mathcal{S}(\mathbf{R})$ is defined by $\widehat{(I^\alpha \varphi)}(\gamma) = |\gamma|^{-\alpha} \varphi(\gamma)$, thus the identity (29) can be rewritten as

$$\rho(t) = \frac{1}{2} I^{-1}(R_\omega \psi)(t).$$

Extend ρ to a function in the space of lines by making it independent of the slope of the line, $\rho(\omega, t) = \rho(t)$ for every $\omega \in S^1$, then we have

$$R^\# \rho(x) = \frac{1}{2} R^\# I^{-1} R_\omega \psi(x) = \psi(x)$$

since the last formula is a rewritting of formula (16) in terms of the Riesz transform. More generally, for any $a > 0$ and every $\omega \in S^1$, we have

$$(R^\# D_a \rho_\omega)(x) = a^{1/2} D_a \check{\psi}(x),$$

so that, using identity (14) and the fact that ρ is real valued, we obtain

$$\begin{aligned} W_\psi f(a,x) &= (f * D_a \check{\psi})(x) \\ &= a^{-1/2} (f * R^\# D_a \check{\rho}_\omega)(x) \\ &= a^{-1/2} R^\# (R_\omega f \otimes D_a \check{\rho}_\omega)(x) \\ &= a^{-1/2} \int_{S^1} (W_\rho R_\omega f)(a, x \cdot \omega) dw \end{aligned}$$

This concludes the proof of the proposition. ∎

A similar relation between the Radon transform and the CWT can be found using "separable" wavelets in $\mathbf{R}^2$.

Proposition 2. Given a separable 2-dimensional wavelet of the form

$$\psi(x) = \psi^1(x_1)\psi^2(x_2)$$

where each $\psi^i(t)$ satisfies $|\hat{\psi}^i(\gamma)| \leq C_1(1+|\gamma|)^{-1}$ for all $\gamma \in \mathbf{R}$, define the family of one-dimensional functions $\{\rho_\omega\}_{\omega \in S^1}$ by

$$\hat{\rho_\omega}(\gamma) = \frac{1}{2}|\gamma|\hat{\psi}^1(\gamma\omega_1)\hat{\psi}^2(\gamma\omega_2)$$

where $\omega = (\omega_1, \omega_2) \in S^1$. Then, for every $f \in L^1(\mathbf{R}^2) \cap L^2(\mathbf{R}^2)$,

$$(W_\psi f)(a,x) = a^{-1/2} \int_{S^1} (W_{\rho_\omega} R_\omega f)(a, x \cdot \omega) d\omega.$$

The point of Proposition 2 is the observation that the wavelet transform of a function $f(x)$ with any mother wavelet and at any scale and location can be obtained by backprojecting the wavelet transform of the Radon transform of f using wavelets that vary with each angle, but which are admissible for each angle.

So far we have not yet shown that the inversion formulas of the Radon transform based on wavelets do a good localization job. Using Proposition 1 the problem is clear, find a function ρ such that ρ has small support and simultaneously ψ has small support. From the relation (29) we see that we have overcome the Reisz operator of order -1, its symbol is $|\gamma| = (\text{sgn}\gamma)\gamma$, so it is the composition of the differentiation and the Hilbert transform. (This is exactly the content of the inversion formula (18).) The problem, of course, is the Hilbert transform, but if we choose ρ with many vanishing moments, then we can overcome the difficulty. For the sake of comparison we show in Figure 3 the Hilbert transform of a Gaussian, its effective support is about four times the effective support of the Gaussian (defined by making zero those points below 1% of maximum value), which tails exactly with the result about the interior Radon transform mentioned earlier in this section.

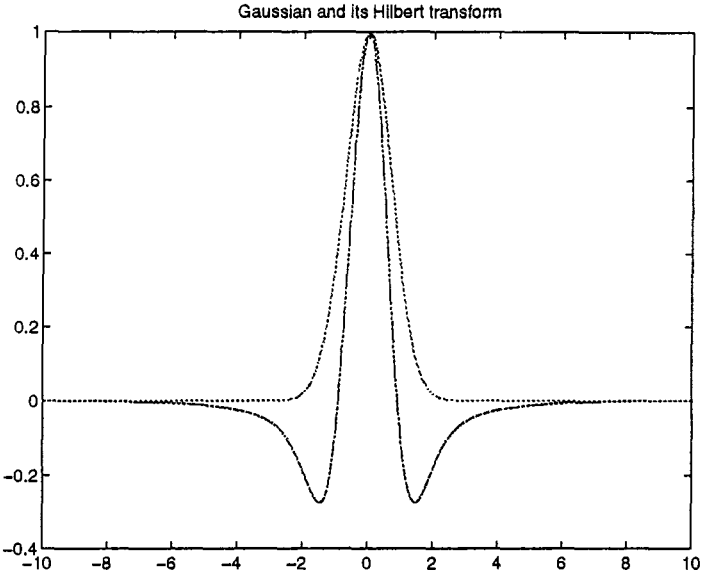

Figure 3: Gaussian and its Hilbert transform.

The key to explain the success of the wavelet method of localization is the following proposition [BW1], which in spirit is similar to the general principles about Calderon-Zygmund operators stated in [BCR].

Proposition 3. Suppose that n is an even integer and the compactly supported function $h \in L^2(\mathbf{R})$ is such that for some integer $m \geq 0$ we have that $\hat{h}$ is $n+m-1$ times differentiable and satisfies

(a) $\gamma_j \hat{h}^{(k)}(\gamma) \in L^1(\mathbf{R}) \cap L^2(\mathbf{R}) \qquad$ for $0 \leq j \leq m, 0 \leq k \leq m+n-1$

(b) $\int_{-\infty}^{\infty} t^j h(t)dt = 0 \qquad$ for $0 \leq j \leq m$

Then

$$I^{1-n}h(t) = o(|t|^{-n-m+1}) \text{ as } |t| \to \infty$$

and

$$t^{n+m-1} I^{1-n} h \in L^2(\mathbf{R}).$$

The proof is rather elementary, it depends on the fact that if h is a function of compact support with $m+1$ vanishing moments then $|\gamma|^{n-1}\hat{h}(\gamma)$ has $n+m-1$ continuous derivatives.

For ease of application it is better to work with the *discrete wavelet transform* (DWT). This is basically obtained by discretizing the CWT or appealing to the multiresolution analysis of Mallat and Meyer [D], [M]. We have done this in detail in [FLBW] using coiflets [D] in order to be able to implement the inversion process using filter banks. One can show that to obtain a relative error of 0.5% one only needs a margin of security of 12 pixels around the region of interest (ROI). For instance, to recover within this error bound an image occupying a disk of radius 20 pixels in a 256×256 image, one only needs about 25% of exposure, as shown in Figure 4.

Figure 5 below is the Shepp-Logan phantom and its reconstruction from global fan beam data using the standard algorithm, in Figure 6 we use local data and our wavelets algorithm.

The following figures are the reconstruction of a heart from real CAT scanner data using our wavelet method, and the reconstruction of the central part from local data and our wavelet method is found below.

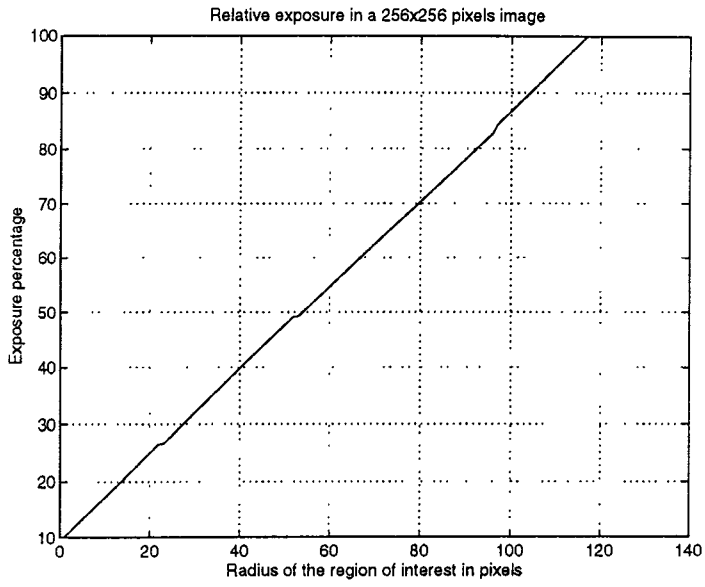

Figure 4: Exposure versus the radius of the ROI.

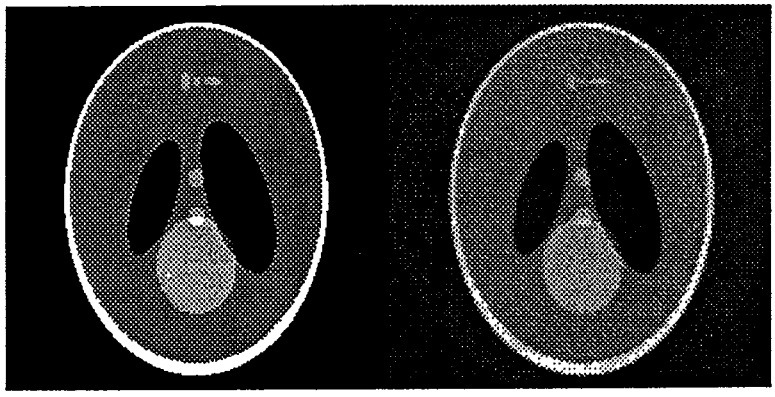

(a) (b)

Figure 5: (a) The Shepp-Logan head phantom; (b) the standard filtered backprojection in fan beam geometry (4).

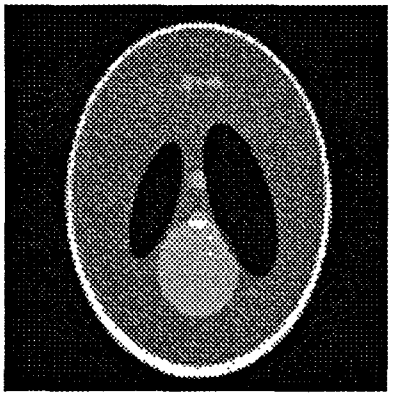

Figure 6: Reconstruction from wavelet coefficients.

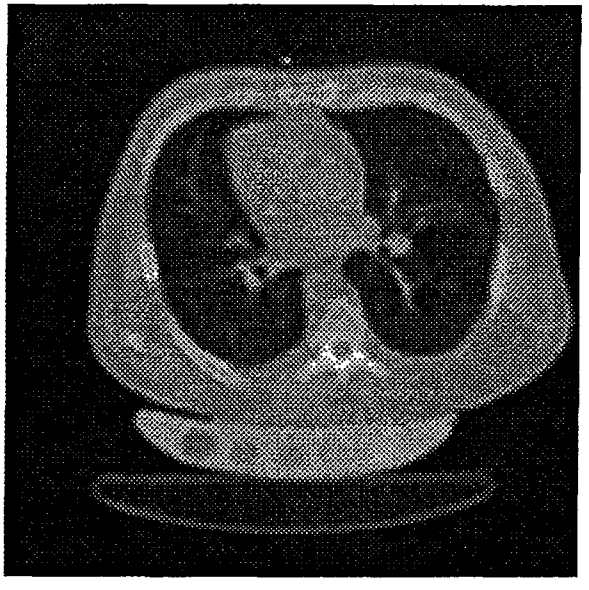

Figure 7: Reconstruction of heart from wavelet coefficients.

Figure 8: The local reconstruction of of central portion of heart.

We leave to the discussion and references in [FLBW] and [BW2] the comparison with other methods of inversion of the Radon transform using wavelets. One should add to the references in those two papers, the very recent work of Rubin [R], which is based on a systematic use of the Calderon reproducing formula and it is thus a development of the original ideas in [Ho].

4. The hyperbolic Radon transform and Electrical Impedance Tomography

In this section we discuss the role tomography plays in a classical problem of Applied Mathematics, the inverse conductivity problem. Several of the earlier attempts to solve this problem involve generalizing the Radon transform to other geometries, that is, integrating functions over other families of curves beyond straight lines in the Euclidean plane. There are many examples of such transforms, in fact, the integration over great circles in S^2 was a transform considered by Minkowski and which inspired Radon in his work. The two we shall introduce presently are the generalized Radon transform of Beylkin [By] and the Radon transform on the hyperbolic plane [Hel].

Let Ω be an open subset of $\mathbf{R}^2$ and $\phi \in C^\infty(\Omega \times (\mathbf{R}^2 \setminus \{0\}))$ be such that

(a) $\phi(x, \lambda\xi) = \lambda\phi(x, \xi)$ for $\lambda > 0$

(b) $\bigtriangledown_x \phi(x, \xi) \neq 0$ for all $(x, \xi) \in \Omega \times (\mathbf{R}^2 \setminus \{0\})$

Then, for any $s \in \mathbf{R}$ and $\omega \in S^1$ we can define the smooth curve

$$H_{s,\omega} = \{x \in \Omega : \phi(x, \omega) = s\},$$

that is, the level curves of ϕ. We let $d\sigma$ denote the Euclidean arc length in such a curve. For $u \in C_0^\infty(\Omega)$ define the "Radon transform"

$$R_\phi u(\omega, s) = \int\limits_{H_{s,\omega}} u(x) | \bigtriangledown_x \phi(x, \xi)| d\sigma(x)$$

Let $h(x, \xi)$ be the Hessian determinant of ϕ with respect to the second variables, $h(x, \xi) = \det[\frac{\partial^2 \phi(x,\xi)}{\partial \xi_j \partial \xi_k}]$, then the "backprojection" operator $R_\phi^\#$ is defined by

$$R_\phi^\# v(x) = \int\limits_{\omega \in S^1} \frac{h(x, \omega)}{| \bigtriangledown_x \phi(x, \xi)|^2} v(\omega, \phi(x, \omega)) dw$$

Introducing K as the operator of convolution by $1/|x|$, Beylkin proved the following approximate inversion formula for the Radon transform as an operator

$$R_\phi : L^2_c(\Omega) \to L^2_{\text{loc}}(\Omega),$$

namely,

$$R^{\#}_\phi K R_\phi = I + T \tag{30}$$

where, I is the identity map and

$$T : L^2_c(\Omega) \to L^2_{\text{loc}}(\Omega)$$

is a compact operator. In fact, Beylkin gives a recipe for a family of back-projection operators and generalized convolution operators K so that a decomposition of the type (30) holds. This gives his transform great flexibility and applicability to many problems, especially inverse acoustic problems, of course, the reader can easily verify that for convenient choices of ϕ, the transform R_ϕ yields the Euclidean Radon transform studied earlier and the hyperbolic one, which we now introduce. (The reader should consult [He1], [He3] for more details on this subject.)

Let D, the unit disk of the complex plane $\mathbf{C}$, be endowed with the hyperbolic metric of arc-length element ds given by

$$ds^2 = \frac{4|dz|^2}{(1-|z|^2)^2}, \tag{31}$$

where $|dz|$ denotes the Euclidean arc-length element.

This metric is clearly conformal to the Euclidean metric but has constant curvature -1. The geodesics of this metric are the diameters of D and the segments lying in D of the Euclidean circles intersecting the unit circle ∂D perpendicularly. One can introduce geodesic polar coordinates $z \leftrightarrow (\omega, r)$, where $\omega = z/|z|, r = d(z,0)$. Note that $|z| = \tanh(r/2)$. In these coordinates the metric (31) can be rewritten as

$$ds^2 = dr^2 + \sinh^2 r \, d\omega^2$$

where $d\omega^2$ indicates the usual metric on ∂D. The hyperbolic distance between two points is given by

$$d(z,\omega) = \text{ arcsinh } (\frac{|z-w|}{(1-|z|^2)^{1/2}(1-|w|^2)^{1/2}}).$$

The Laplace-Beltrami operator Δ_H on D can be written in terms of the Euclidean Laplacian Δ as

$$\begin{aligned} \Delta_H &= \frac{(1-|z|^2)^2}{4}\Delta \\ &= \frac{\partial^2}{\partial r^2} + \coth r \frac{\partial}{\partial r} + \sinh^{-2} r \frac{\partial^2}{\partial \omega^2}. \end{aligned} \tag{32}$$

The classical Moebius group of complex analysis is the group of orientation preserving isometries of the hyperbolic plane D.

One can define the hyperbolic Radon transform R_H by

$$Rf(\gamma) = R_H f(\gamma) = \int_\gamma f(z) ds(z), \gamma \text{ geodesic in } D \tag{33}$$

which is well defined for, say, continuous functions of compact support, or functions decaying sufficiently fast. Observe that to be integrable on the hyperbolic ray $[0,\infty[$ (which is just the straight line segment from 0 to 1 in the complex plane $\mathbf{C}$), f has to decay a bit faster than e^{-r}. We denote by Γ the space of all geodesics in D, then the dual transform $R^\#$ (or backprojection operator) is given by

$$R^\# \phi(z) = \int_{\Gamma_z} \phi(\gamma) d\mu_z(\gamma), \tag{34}$$

where Γ_z is the collection of geodesics through the point z and $d\mu_z$ is the normalized measure of Γ_z. Since a geodesic through z is determined by its starting direction $\omega \in S^1$, then $\Gamma_z \approx S^1$ and $d\mu_z$ is naturally associated to $\frac{1}{2\pi} d\omega$ when we use this particular parameterization of Γ_z.

In order to invert R_H one can proceed in the spirit of Radon's inversion formula (19). This was done by Helgason [He2, p. 155]. Or one can try to find a filtered backprojection type formula like (16). For that purpose we need to define *convolution operators* with respect to a radial kernel k. For $k \in L^1_{\text{loc}}([0,\infty))$ and $f \in C_0(D)$ we define

$$k * f(z) = k *_H f(z) := \int_D f(w)k(d(z,w))dm(w) \tag{35}$$

where $dm(w)$ stands for the hyperbolic area measure, which in polar coordinates is given by

$$dm = \sinh r \, dr d\omega.$$

Corresponding to the Euclidean formula (15) we have

$$R_H^{\#} R_H f = k * f, \text{ where } k(t) = \frac{1}{\pi \sinh t} \tag{36}$$

One can prove [BC1] that if

$$S(t) = \coth t - 1 \tag{37}$$

then

$$\frac{1}{4\pi} \Delta_H S *_H R_H^{\#} R_H = I \tag{38}$$

which is the exact analogue of (16).

It is convenient to recall here that in the hyperbolic disk D we have a Fourier transform [He2]. It is easier to work it out for "radial" functions as we interpret our kernel k, then the Fourier transform is defined with the help of the Legendre functions $P_\nu(r)$ by means of the following formula

$$\hat{k}(\lambda) = 2\pi \int_0^\infty k(t) P_{i\lambda - 1/2}(\cosh t) \sinh t dt \qquad (\lambda \in \mathbf{R})$$

For radial functions k, m, we have

$$\widehat{(k * m)}(\lambda) = \hat{k}(\lambda)\hat{m}(\lambda)$$

So that, if $\hat{k}(\lambda) \neq 0$ for all $\lambda \in \mathbf{R}$, in principle, that is, for a convenient class of functions f, the convolution operator $f \longmapsto k *_H f$ is invertible.

We refer to [He2], [BC1], [BC2], [Ku] for corresponding inversion formulas in the higher dimensional hyperbolic spaces, and the characterization of the range of the Radon transform. In particular, [Ku], [BC2] exploit the

"intertwining" between R_H and the Euclidean Radon transform as well as the Minkowski-Radon transform on spheres.

Let us explain now what the above hyperbolic Radon transform has to do with Electrical Impedance Tomography (EIT) and what EIT is.

Let us consider the following tomographic problem: using a collection of electrodes of the type used in electrocardiograms (EKG) uniformly distributed around the breast of a patient and all lying in the same plane, introduce successively (weak) currents at each one of the electrodes (as done in EKG) and measure the induced potential at the remaining ones. The objective is to obtain an image of a cross section of the lungs to determine whether there is a collapsed lung or not. This was what Barber and Brown set up to do in 1984 [BB1], [BB2]. The point being that this equipment is cheap, transportable and provides a non-intrusive test (that is, no punctures have to be done to the chest cavity). Similarly, one can try to determine the rate of pumping of the heart using this kind of equipment. Note that the pulse only determines the rate of contracting and expanding of the heart but not how much blood is being pumped by it. Another completely different problem arises in the determination of the existence and lengths of internal cracks in a plate, by using electrostatic measurements on the boundary [FV], [BCW], [W]. These three are examples of the following inverse problem. (The best reference for the general facts about this problem is the supply [SU]. See also the nice explanation for the general public [C], [S]):

Assume β is a strictly positive (nice) function in the closed unit disk $\bar{D}$. If we were to introduce a current at the boundary ∂D, represented by a function ψ satisfying $\int_{\partial D} \psi ds = 0$, then the Neumann problem

$$\begin{cases} \text{div } (\beta \text{ grad } u) & = 0 \text{ in } D \\ \beta \frac{\partial u}{\partial n} & = \psi \text{ on } \partial D \end{cases} \tag{39}$$

has a solution u which is unique up to an additive constant. If ψ is a nice function then $\frac{\partial u}{\partial s}$ (that is, the tangential derivative of u) is well defined on ∂D, so we have the input-output map

$$\Lambda_\beta : \psi \longmapsto \frac{\partial u}{\partial s}$$

which is a linear continuous map from the Sobolev space $H^\alpha(\partial D)$ into itself. (This statement holds for any domain D with nice boundary, not just the disk.)

Consider now the (very non-linear) map

$$\beta \longmapsto \Lambda_\beta \tag{40}$$

is it injective? Can one find the inverse to this map? This problem was originally posed by A. Calderón, who proved that (40) was locally invertible near $\beta =$ constant, more recently Nachman [N1], [N2] proved global invertibility. Since β is usually called the conductivity and $1/\beta$ the impedance, this is the reason for the name EIT of this inverse problem. In the biological applications we know the value β for the different constituents like blood, lung tissue, etc., so one only looks for a profile of the areas occupied by them. In the determination of cracks, one can assume β "known", except for curves where $\beta = 0$, and one wants to determine this curve, or whether any exists. One can find in [SU] many important inverse problems that are equivalent to EIT: in acoustics, radiation scattering, etc. Note that in the problem of the rate of pumping of the heart, we can think that all we want to determine is just a single number, this rate. Isaacson, Newell and collaborators have in fact patented [C], [I] a device that measures this rate with the help of EIT. We also know that this problem, being an inverse elliptic problem is very ill-conditioned, so in any case one is willing to restrict oneself to find the deviation of β from an assumedly known conductivity β_0. In the simplest case we assume $\beta_0 \equiv 1$, so that $\beta = 1 + \delta\beta, |\delta\beta| << 1$, and we further assume $\delta\beta = 0$ on ∂D (One can always reduce matters to this case). Thus $u = U + \delta U$, where U is the solution of (39) for the same boundary value, and $\beta = 1$. In other words

$$\begin{cases} \Delta U &= 0 \quad \text{in } D \\ \frac{\partial U}{\partial n} &= \psi \quad \text{on } \partial D \end{cases} \tag{41}$$

Here Δ is the Euclidean Laplacian. The perturbation δU then satisifes

$$\begin{cases} \Delta(\delta U) &= - < \text{grad } (\delta\beta), \text{grad } U > \text{ in } D \\ \frac{\partial(\delta U)}{\partial n} &= -(\delta\beta)\psi \qquad\qquad\qquad \text{on } \partial D \end{cases} \tag{42}$$

We have at our disposal the choice of inputs ψ. Their only restriction is that $\int_{\partial D} \psi ds = 0$. For that reason, they can be well approximated by linear combinations of dipoles. A dipole at a point $\omega \in \partial D$ is given by $-\pi \frac{\partial}{\partial s} \delta_\omega$.

It turns out that the solution U_ω of

$$\begin{cases} \Delta U_\omega &= 0 & \text{in } D \\ \frac{\partial U_\omega}{\partial n} &= -\pi \frac{\partial}{\partial s}\delta_\omega & \text{on } \partial D \end{cases} \tag{43}$$

has level curves which are arcs of circles passing through ω and perpendicular to ∂D. That is, the level curves of U_ω are exactly the geodesics of the hyperbolic metric. This fact passd unnoticed to Barber and Brown but they definitely realized that the value

$$\mu = \frac{\partial(\delta U)}{\partial s} \tag{44}$$

at a point $a' \in \partial D$ must be some sort of integral of $\delta\beta$ over the level curve of U_ω that ends at a, precisely the geodesic starting at ω and ending at a. In other words, μ is a function in the space of geodesics in D considered as the hyperbolic plane, all the geodesics are obtained this way by changing ω and a. Without expressly stating this, Barber and Brown introduced a "backprojection" operator that turned out to be exactly $R_H^\#$ and gave the approximation to $\delta\beta$ as $R_H^\#\mu$. Santosa and Vogelius recognized explicitly that some sort of Radon transform was involved and used the generalized Byelkin transform and a convenient choice of K in (30) to stabilize numerically the inversion of EIT. Casadio and I, prodded by a question of Santosa and Vogelius, saw that R_H was involved and developed the inversion formula (38) for this purpose. As it turns out, all of these approaches are just *approximations* to the linearized problem. Only in [BC3], [BC4], we realized the fact that the *exact* formulation of the linearized problem in terms of hyperbolic geometry requires also a convolution operator! Namely, let

$$\kappa(t) = \frac{\cosh^{-2}(t) - 3\cosh^{-4}(t)}{8\pi} \tag{45}$$

and μ the boundary data (44) considered as a function on the space of geodesics in D, then one has that the exact relation between $\delta\beta$ and μ is given by

$$R_H(\kappa *_H \delta\beta) = \mu \tag{46}$$

Using the backprojection operator we also obtain

$$R_H^\#\mu = R_H^\# R_H(\kappa *_H \delta\beta) \tag{47}$$

so that

$$\frac{1}{4\pi}\Delta_H(S *_H (R_H^{\#}\mu)) = \kappa *_H \delta\beta \tag{48}$$

which requires to invert the convolution operator of symbol κ. One can compute its hyperbolic Fourier transform $\hat{\kappa}$ exactly and find out that $\hat{\kappa}(\lambda) \neq 0$ for every $\lambda \in \mathbf{R}$, so that the operator $\kappa*$ is, in principle, invertible, but the numerical implementation of this inversion has proven difficult so far. (Although Kuchment and his students have made in [FMLKMLPP] some progress towards implementing a numerical Fourier transform in D, which we hope will prove useful to compute $\delta\beta$.) One can recognize in (47) and (48) the same principle that lead to the numerical approach in [BB1], [SV] and others. Due to the importance of this problem there have been many other interesting approximate inversion formulas, under special assumptions on the conductivity β, for instance, β is "blocky", that is the linear combination with positive coefficients of a finite number of disjoint squares [DS]. Their approach is variational, and one may wonder whether one could not use some version of the Mumford-Shah edge detection algorithms [MS] to obtain a rather sharp solution of the inverse conductivity problem (40).

5. Final remark

The objective of these short notes (and the corresponding CIME course) was only to indicate how, beyond the well-known applications of tomography to Medicine, there are many other possible ones. Moreover, even to solve them approximately, they require deep mathematical tools, showing once more that the applicability of "pure" and "abstract" mathematics is not a fairy-tale but a concrete reality. It also indicates that it pays to "invest" one's time trying to communicate with those, be they physicists, or physicians, etc., that have the ready made applications. A lesson often lost by graduate students in Mathematics.

6. References

[**AA**] S. Andrieux and A Ben Alda, Identification de fissures planes par une donnée de bord unique, C.R. Acad. Sci. Paris 315 I(1992), 1323-1328.

[**AU**] A. Aldroubi and M. Unser, editors, "Wavelets in Medicine and Biology," CRC Press, 1966, 616 pages.

[**BB1**] D. C. Barber and B. H. Brown, Recent developments in applied potential, in "Information processing in Medical Imaging," S. Bacharach (ed.), Martinus Nijhoff, 1986, 106-121.

[**BB2**] D. C. Barber and B. H. Brown, Progress in Electrical Impendance Tomography, in "Inverse problems in partial differential equations," D. Colton et al. (eds.), SIAM, 1990, 151-164.

[**BC1**] C. A. Berenstein and E. Casadio Tarabusi, Inversion formulas for the k-dimensional Radon transform in real hyperbolic spaces, Duke Math. J. 62 (1991), 613-632.

[**BC2**] C. A. Berenstein and E. Casadio Tarabusi, Range of the k-dimensional Radon transform in real hyperbolic spaces, Forum Math. 5 (1993), 603-616.

[**BC3**] C. A. Berenstein and E. Casadio Tarabusi, The inverse conductivity problem and the hyperbolic x-ray transform, in "75 years of Radon transform," S. Gindikin and P. Michor, editors, International Press, 1994, 39-44.

[**BC4**] C. A. Berenstein and E. Casadio Tarabusi, Integral geometry in hyperbolic spaces and electrical impedance tomography, SIAM J. Appl. Math. 56 (1996), 755-764.

[**BCW**] C. A. Berenstein, D. C. Chang and E. Wang, A nondestructive inspection method to detect a through crack by electrostatic boundary measurements, ISR-TR 96-1.

[**BW1**] C. A. Berenstein and D. Walnut, Local inversion of the Radon transform in even dimensions using wavelets, in "75 years of Radon transform," S. Gindikin and P. Michor, editors, International Press, 1994, 45-69.

[BW2] C. A. Berenstein and D. Walnut, Wavelets and local tomography, in "Wavelets in Medicine and Biology," A. Aldroubi and M. Unser, editors, CRC Press, 1966.

[BQ] J. Boman and E. Quinto, Support theorems for real analytic Radon transforms, Duke Math. J. 55 (1987), 943-948.

[BV] K. M. Bryan and M. Vogelius, A computational algorithm to detect crack locations from electrostatic boundary measurements, Int. J. Eng. Sci. 32 (1994), 579-603.

[By] G. Beylkin, The inversion problem and applications of the generalized Radon transform, Comm. Pure Appl. Math. 37 (1984), 579-599.

[BCR] G. Beylkin, R. Coifman, and V. Rokhlin, Fast wavelet transforms and numerical algorithms I, Comm. Pure Appl. Math. 44 (1991), 141-183.

[C] B. Cipra, Shocking images from RPI, SIAM News, July 1994, 14-15.

[D] I. Daubechies, "Ten lectures on wavelets," SIAM, 1992.

[DB] A.H. Delaney and Y. Bresler, Multiresolution tomographic reconstruction using wavelets, ICIP-94, 830-834.

[DO] J. DeStefano and T. Olson, Wavelet localization of the Radon transform, IEEE Trans. Signal Proc. 42, August 1994.

[DS] D. C. Dobson and F. Santosa, An image enhancement technique for electrical impedance tomography, Inverse Problems 10 (1994), 317-334.

[FRK] A. Faridani, E. Ritman and K. T. Smith, Local tomography, SIAM J. Applied Math. 52 (1992), 1193-1198.

[FLBW] F. Rashid-Farrokhi, K. J. R. Liu, C. A. Berenstein and D. Walnut, Wavelet-based multiresolution local tomography, ISR-TR 95-73, see also ICIP-95, Washington, DC.

[FLB] F. Rashid-Farrokhi, K. J. R. Liu and C. A. Berenstein, Local tomography in fan-beam geometry using wavelets, ICIP-96, Laussane.

[**FMP**] B. Fridman, D. Ma, and V. G. Papanicolau, Solution of the linearized inverse conductivity problem in the half space, preprint Wichita St. U., 1995.

[**FMLKMLPP**] B. Fridman, D. Ma, S. Lissianoi, P. Kuchment, M. Mogilevsky, K. Lancaster, V. Papanicolaou, and I. Ponomaryov, Numeric implementation of harmonic analysis on the hyperbolic disk, in preparation.

[**FV**] A. Friedman and M. Vogelius, Determining cracks by boundary measurements, Indiana U. Math. J. 38 (1989), 527- 556.

[**GG**] I. M. Gelfand and S. Gindikin, editors, "Mathematical problems of tomography," AMS, 1990.

[**GM**] S. Gindikin and P. Michor, editors, "75 years of Radon transform," International Press, 1994.

[**GIN**] D. Gisser, D. Isaacson, and J. Newell, Current topics in impedance imaging, Clin. Phys. Physiol. 8 (1987), 216-241.

[**GS**] V. Guillemin and S. Sternberg, "Geometric asymptotics," AMS, 1977.

[**He1**] S. Helgason, "The Radon transform," Birkhäuser, 1980.

[**He2**] S. Helgason, "Groups and geometric analysis," Academic Press, 1984.

[**He3**] S. Helgason, "Geometric analysis on symmetric spaces," AMS, 1994.

[**Ho**] M. Holschneider, Inverse Radon transform through inverse wavelet transforms, Inverse Problems 7 (1991), 853-861.

[**J**] F. John, "Plane waves and spherical means," Springer-Verlag, reprinted from originial edition Interscience, 1955.

[**Ka**] G. Kaiser, A friendly guide to wavelets, Birkhäuser, 1994.

[**KS**] A. C. Kak and M. Slaney, "Principles of computerized tomographic imaging," IEEE Press, 1988.

[**KaS**] P. G. Karp and F. Santosa, Non-destructive evaluation of corrosion damage using electrostatic measurements, preprint 1995.

[KR] A. I. Katsevich and A. G. Ramm, New methods for finding values of jump of a function from its local tomography data, Inverse Probl. 11 (1995), 1005-1023.

[Ke] F. Keinert, Inversion of k-plane transforms and applications in computer tomography, SIAM Riview 31 (1989), 273-289.

[KLM] P. Kuchment, K. Lancaster and L. Mogilevskaya, On local tomography, Inverse Problems 11 (1995), 571-589.

[KSh] P. Kuchment and I. Shneiberg, Some inversion formulas for SPECT, Applicable Analysis 53 (1994), 221-231.

[Ku1] A. Kurusa, The Radon transform on hyperbolic space, Geometriae Dedicata 40 (1991), 325-336.

[Ku2] A. Kurusa, Support theorems for the totally geodesic Radon transform on constant curvature spaces, Proc. Amer. Math. Soc. 122 (1994), 429-435.

[M] Y. Meyer, "Ondelettes et opérateurs," 3 vols., Herman, 1990.

[MS] J. M. Morel and S. Solimini, "Variational methods in image segmentation," Birkhäuser, 1995.

[N1] A. I. Nachman, Reconstruction from boundary measurements, Annals Math. 128 (1988), 531-576.

[N2] A. I. Nachman, Global uniqueness for a two-dimensional inverse boundary value problem, Annals Math. 143 (1996), 71-96.

[Na] F. Natterer, "The mathematics of computerized tomography," Wiley, 1986.

[O] T. Olson, Optimal time-frequency projections for localized tomography, Annals of Biomedical Engineering 23 (1995), 622-636.

[Q1] E. T. Quinto, Tomographic reconstruction from incomplete data-numerical inversion of the exterior Radon transform, Inverse Problems 4 (1988), 867-876.

[Q2] E. T. Quinto, Singularities of the X-ray transform and limited data tomography in $\mathbf{R}^2$ and $\mathbf{R}^3$, SIAM J. Math. Anal. 24 (1993), 1215-1225.

[Q3] E. T. Quinto, Computed tomography and rockets, Springer Lecture Notes in Math. 1497 (1991), 261-268.

[QCK] E. T. Quinto, M. Cheney, and P. Kuchment, eds., "Tomography, impedance imaging, and integral geometry," Lect. Appl. Math. 30, Amer. Math. Soc., 1994.

[R] B. Rubin, Inversion and characterization of Radon transforms via continuous wavelet transforms, Hebrew Univ. TR 13, 1995/96.

[RS] A. Ramm and A. I. Zaslavsky, Singularities of the Rdaon transform, Bull. Amer. Math. Soc. 25 (1993), 109-115.

[S] F. Santosa, Inverse problem holds key to safe, continuous imaging, SIAM News, July 1994, 1 and 16-18.

[ST] H. Schonberg and J. Timmer, The gridding method for image reconstruction by Fourier transformation, IEEE Trans. Medical Imaging 14 (1995), 596-607.

[SCII] E. Sommersalo, M. Cheney, D. Isaacson, and I. Isaacson, Layer stripping: a direct numerical method for impedance imaging, Inverse Probl. 7 (1991), 899-926.

[SU] J. Sylvester and G. Uhlmann, The Dirichlet to Neumann map and applications, in "Inverse problems in partial differential equations," D. Colton et al., eds., SIAM, 1990, 101-139.

[SV] F. Santosa and M. Vogelius, A backprojection algorithm for electrical impedance imaging, SIAM J. Appl. Math. 50 (1990), 216-243.

[W] D. Walnut, Applications of Gabor and wavelet expansions to the Radon transform, in "Probabilistic and stochastic methods in analysis," J. Byrnes et al., ed., Kluwer, 1992, 187-205.

[Wa] E. Wang, Ph.D. thesis, University of Maryland, College Park, 1996.

[ZCMB] Y. Zhang, M. A. Coplan, J. H. Moore and C. A. Berenstein, Computerized tomographic imaging for space plasma physics, J. Appl. Phys. 68 (1990), 5883-5889.

Institute for Systems Research
University of Maryland
College Park, MD 20742
carlos@src.umd.edu